

Amplified antimicrobial action of chlorhexidine encapsulated in PDAC-functionalized acrylate copolymer nanogel carriers

Mohammed J. Al-Awady,^{a,b} Paul J. Weldrick,^{a,c} Matthew J. Hardman,^c Gillian M. Greenway,^a and Vesselin N. Paunov^{a*}

Received 00th January 20xx,
Accepted 00th January 20xx

DOI: 10.1039/x0xx00000x

www.rsc.org/MCF

We have developed and tested a novel functionalised nanocarrier for chlorhexidine (CHX) which provides a very strong enhancement of its antimicrobial action. The nanocarrier was based on lightly-cross-linked acrylate copolymer nanogel particles loaded with CHX followed by a surface functionalisation with the cationic polyelectrolyte poly(diallyldimethylammonium chloride (PDAC)). We explored the antimicrobial effect of the PDAC-coated CHX-loaded nanogel carriers on *E. coli*, *S. aureus*, *C. cerevisiae* and *C. reinhardtii* and discovered that it is much higher than that of solution with equivalent overall concentration of free CHX. Our experiments also showed a marked increase of the cationic CHX-loaded nanocarriers antimicrobial action on these microorganisms at shorter incubation times compared with the non-coated CHX-loaded nanogel particles at the same CHX concentration and other conditions. We attribute the increase in the antimicrobial activity of the cationically-functionalised nanogel carrier to its electrostatic adhesion to the microbial cells walls which allows much higher CHX concentration to be delivered directly onto the cell surface. The results of this study can be used for development of novel more efficient antialgal, antifungal and antibacterial formulations based on cationically functionalised nanogels. Our method can also be used for boosting the effect of other cationic antimicrobial agents by encapsulating them in cationically-functionalised nanogel carriers. This nanotechnological approach could lead to developing more effective antimicrobial and disinfecting agents, dental formulations for plaque control, wound dressings, antialgal/antibiofouling formulations and novel antifungal agents.

Introduction

Nanocarrier-based drug delivery is a rapidly evolving area aimed at releasing and maintaining optimal concentrations of nanoparticle-encapsulated therapeutic agents to the specifically target infected tissues, tumours, etc. while reducing their side effects on normal tissues.^{1,2} Commonly used nanocarriers for drug delivery include liposomes, polymeric micelles and dendrimers, artificial DNA structures, and biodegradable scaffolds.² Nanogels are internally cross-linked particles of hydrophilic polymer which may contain sulphate, hydroxyl and carboxyl ionisable groups in polymer chains.³ Such physically or chemically cross-linking polymer networks can swell in a aqueous suspension due to water absorption.⁴⁻⁵ Nanogels have good biocompatibility which is crucial for avoiding inflammatory responses and other side effects.⁶⁻⁸ Chlorhexidine gluconate (CHX) is a cationic bisbiguanide and consists of two symmetric 4-chlorophenyl rings and two

biguanide groups linked by a central hexamethylene chain. CHX digluconate salt is easily soluble in water^{9,10} and is frequently used as a chemotherapeutic agent especially against oral diseases due to its wide spectrum of activity against yeasts, Gram-positive, Gram-negative bacteria and many anaerobic pathogens.¹¹ The CHX cation binds to anionic groups on the bacterial surface such as phosphate groups of teichoic acid in Gram-positive and lipopolysaccharide in Gram-negative bacteria and disrupts their membrane integrity.¹² This leads to leakage of the cell constituents and eventually to the cells death.¹³ CHX is one of the most effective antimicrobial agents for dental plaque control.¹⁴⁻¹⁶ A recent and practical release system is the combination of microfibrillated cellulose (MFC) and β -cyclodextrin (β -CD) that produces a large dosage of chlorhexidine gluconate over a prolonged period of time, MFC is known for its burst action whilst β -CD is a slow releasing drug delivery agent.¹⁷ Mesoporous silica nanoparticles have been recently used as a CHX release system that effectively targets planktonic and biofilm modes of oral pathogens.¹⁸ Silica sub-micrometer size capsules impregnated with 2% CHX and coated with sodium alginate and chitosan have been reported as a better root canal drug against *Enterococcus faecalis* which is a major cause of root canal infections.¹⁹ Antimicrobial strategies combining polymer science and nanotechnology have attracted tremendous interest in the last decade because of their great potential in many applications.^{39,40}

^a School of Mathematics and Physical Sciences (Chemistry), University of Hull, Hull, HU67RX, UK.

^b Department of Chemistry, Physiology, and Pharmacology, Faculty of Veterinary Medicine, The Green University of Qasim, Babylon, Iraq.

^c School of Life Sciences, University of Hull, Hull, HU67RX, UK.

*Corresponding author: Tel: +44 1482 465660; Fax: +44 1482 466410; E-mail: v.n.paunov@hull.ac.uk

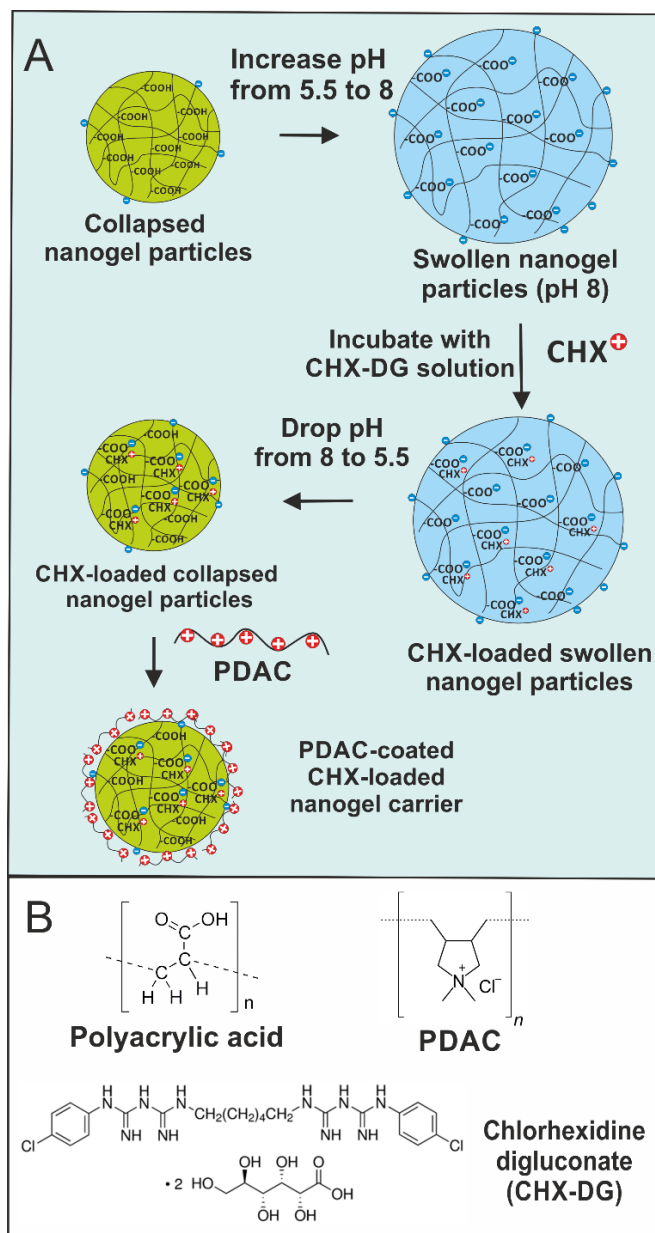


Figure 1. The schematic diagram for the encapsulation of chlorhexidine (CHX) ions from chlorhexidine digluconate) into a Carbolpol nanogels by using swelling/deswelling cycle of the nanogel in the basic (pH 8) and acidic (pH 5.5) medium, respectively. The CHX-loaded nanogel was surface-functionalised with a cationic polyelectrolyte (PDAC). The chemical formulas of the carbomer nanogel (partially crosslinked polyacrylic acid NPs), the PDAC and the chlorhexidine digluconate are also presented.

Poly (dl-lactic-co-glycolic acid) (PLGA) microparticles containing chlorhexidine (CHX) free base, chlorhexidine digluconate (CHX-DG) with methylated- β -cyclodextrin (MBCD) and hydroxypropyl- β -cyclodextrin (HPBCD) have recently been explored against periodontitis causing bacteria (*P. gingivalis* and *B. forsythus*).²⁰

Wound treatment needs molecules that both improve healing and control infection. Poly (lactic-co-glycolic acid) (PLGA) microspheres based drug delivery system for CHX was recently reported which simultaneously transports platelet-derived growth factor (PDGF)-BB, a hydrophilic protein known to stimulate wound healing, and CHX for infection treatment. This

can improve healing and decrease bacteria levels in an infected wound model.²¹ Positively charged CHX-loaded Poly(ϵ -caprolactone) (PCL) nanocapsules, prepared by interfacial polymer deposition /solvent displacement were also reported with good encapsulation efficiency.²² The study described a sustained release of CHX from PCL nanocapsules by mediating a more direct and prolonged contact between the nanocapsules and bacteria, skin surface, and skin follicles and provided a prolonged *ex vivo* topical antimicrobial activity against *Staphylococcus epidermidis*.²²

Antimicrobial nanoparticles (NPs) of hexametaphosphate salt of chlorhexidine (CHX) have been recently produced by co-precipitation of aqueous solutions of CHX digluconate and sodium hexametaphosphate. These NPs adhered well on glass, titanium, and an elastomeric wound dressing surfaces and showed a slow release of CHX over a period of at least 50 days proving effective against methicillin-resistant *S. aureus* (MRSA) and *P. aeruginosa* in both planktonic and biofilm conditions.²³ Recently, nanocarriers formulated from biodegradable materials attracted a lot of attention following concerns about the post-use fate of the nanocarrier formulations.^{24,25} Al-Awady *et al.*²⁶ demonstrated that the nanotoxicity of polyelectrolyte-coated TiO₂NPs changes with the surface charge with those particles with a cationic outer layer (or bare titania nanoparticles at acidic pH) being much more toxic than the ones with an outer layer of anionic polyelectrolyte. A range of other antimicrobial particles have recently been developed which use the same approach for delivery of therapeutic alkaloids.²⁷ Frangville *et al.*²⁸ developed biodegradable lignin nanoparticles which showed no measurable toxicity against proxy organisms like yeast and microalgae. Recently, these were utilised for silver ion delivery system based on Ag⁺-loaded lignin nanoparticles which were further coated with cationic polyelectrolyte.^{29,30} The produced silver ion delivery vehicles proved to more efficient antimicrobial agents for a range of bacteria than equivalent concentrations of silver in metallic silver nanoparticles.

In this study, we push forward these ideas to encapsulate CHX in nanogel particles based on a partially cross-linked acrylate copolymer for antibacterial, antifungal and anti-algal applications. We explore the stability of the CHX-loaded Carbolpol nanogel particles (CLC), the CHX encapsulation efficiency, the controlled release of encapsulated CHX-cations and the antimicrobial activity of the formed CHX-nanogel complexes before and after surface functionalisation with cationic polyelectrolyte. Carbolpol Aqua SF1 is an aqueous dispersion approximately 30% w/v of a lightly cross-linked and highly hydrophilic acrylate nanogel which does not exhibit toxicity against a range of microorganisms and does not trigger inflammatory reactions in animal organs.³¹

Figure 1 explains the encapsulation steps of CHX into the nanogel and the surface functionalisation of the produced nanoparticles with a cationic polyelectrolyte. The retention of the CHX in the core of the nanogel is based on electrostatic interaction with non-covalent bonding to ensure further release of the antimicrobial agent upon incubation of the loaded nanogel particles with the tested microorganisms.

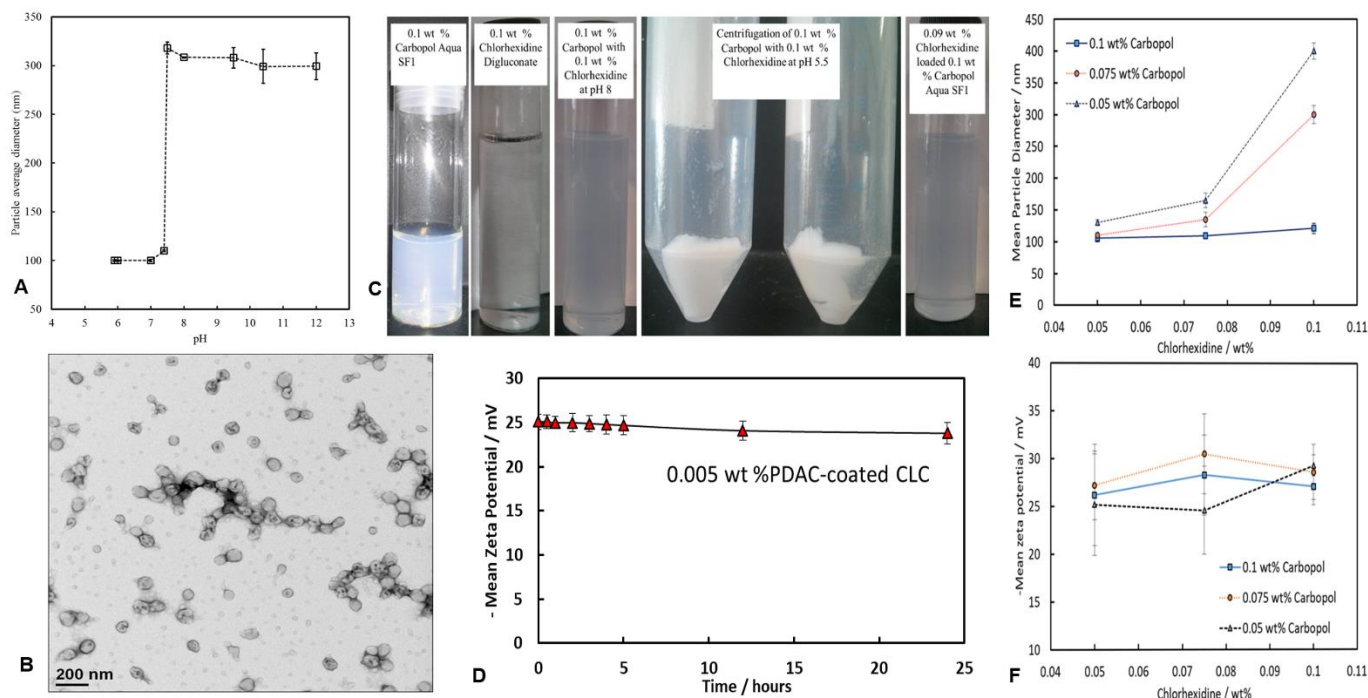


Figure 2. (A) The average particle diameter of Carbopol Aqua SF1 as a function of pH. (B) TEM image of CHX-loaded collapsed Carbopol at pH 5.5 which shows the physical size of the produced collapsed nanogel particles after evaporation of the aqueous media. The encapsulation was achieved through adjusting Carbopol suspension to pH 8, addition of CHX solution to form chlorhexidine-loaded swollen Carbopol. The formed suspension was adjusted to pH 5.5 to “collapsed” CHX loaded Carbopol nanogel (CLC). (C) Photograph of bare Carbopol Aqua SF1 suspension, chlorhexidine solution, CHX-loaded Carbopol at pH 8 and pH 5.5 along with a centrifuged CLC particles and the CLC suspension after re-dispersing it at pH 8. (D) Stability of PDAC-coated Carbopol at pH 5.5. A Malvern Mastersizer was used to measure the zeta potential was measured at time intervals at a refractive index of 1.450. Each value represents a triplicate with \pm SD. (E) The particle hydrodynamic diameter and (F) the mean zeta potential of the CLC particles as a function of the CHX concentration at different concentrations of the Carbopol Aqua SF1.

Here we studied the antibacterial, anti-fungal and anti-algal action of CLC on four proxy microorganisms, *E. coli*, *S. aureus*, *S. cerevisiae* and *C. reinhardtii* respectively. We also study the CHX release kinetics and the boost of its antimicrobial action after coating of the CLC nanocarriers. We show that this strategy can strongly amplify the antimicrobial action of CHX compared to equivalent concentration of free CHX. This versatile and inexpensive nanocarrier can potentially be used for many other cationic antimicrobial agents and antibiotics to provide a boost of their action or minimize their overall concentration.

Materials and Methods

Materials

We used Carbopol Aqua SF1™ nanogel as an aqueous suspension (30 wt%) as supplied by Lubrizol, USA. Fluorescein diacetate (FDA, 98%) for cell viability assays and poly(diallyldimethylammonium chloride) (PDAC) was supplied from Sigma Aldrich, UK. Chlorhexidine digluconate (98%) and was delivered by Fluka, UK. *Chlamydomonas Reinhardtii* (cc-124 strain), was sourced from Flickinger’s group at North Carolina State University, USA). It is a microalgae culture which was grown in Tris-Acetate-Phosphate (TAP) culture medium with an incubation temperature of 30 °C. The culture media for *C. reinhardtii* consisted of TAP salts (NH_4Cl ; $\text{MgSO}_4 \cdot 7\text{H}_2\text{O}$ and $\text{CaCl}_2 \cdot 2\text{H}_2\text{O}$), phosphate buffer solution (PBS) and Hunter’s trace

elements solution (EDTA disodium salt, $\text{ZnSO}_4 \cdot 7\text{H}_2\text{O}$, H_3BO_3 , $\text{MnCl}_2 \cdot 4\text{H}_2\text{O}$, $\text{CoCl}_2 \cdot 6\text{H}_2\text{O}$, $\text{CuSO}_4 \cdot 5\text{H}_2\text{O}$, $\text{FeSO}_4 \cdot 7\text{H}_2\text{O}$, $(\text{NH}_4)_6\text{Mo}_7\text{O}_{24} \cdot 4\text{H}_2\text{O}$, all purchased from Sigma-Aldrich, UK. The microalgae batch was grown in the TAP media at pH 7 while being illuminated for 72 hours with a white luminescent lamp with a light intensity of 60 W m^{-2} under constant stirring with a magnetic stirrer.^{32,33} The stock cultures of *C. reinhardtii* which were used for testing were with typical concentration 4×10^5 cells per mL determined by automatic cell counter (Cellometer Auto X4) and the *E. coli* bacterial culture stock was with approximately 5×10^7 cells per mL. Deionised water purified by reverse osmosis and ion exchange from a Milli-Q water system (Millipore, UK) was used in all our studies. Its surface tension was 71.9 mNm^{-1} at 25 °C, with measured resistivity of 18 M Ω cm.

Preparation of CHX-loaded Carbopol nanogel particles (CLC)

The method is based on a pH induced swelling-deswelling cycle. A 0.1 wt.% aqueous dispersion of the nanogel was prepared by weighing 0.1 g of stock solution of the Carbopol Aqua SF1 and dispersing it in 75 mL Milli-Q water, this was then adjusted to pH 8 using 3 drops of 0.25 M NaOH. An aliquot of 0.1 wt. % of chlorhexidine digluconate was then added dropwise to the Carbopol Aqua SF1 solution to prepare a 0.1 wt. % chlorhexidine in 0.1 wt. % nanogel dispersion. CHX-Carbopol solutions was reduced to pH 5.5 using drops of 0.25 M HCl whilst being stirred for 30 minutes. Solutions was the centrifuged at 8500 rpm for 30 minutes.

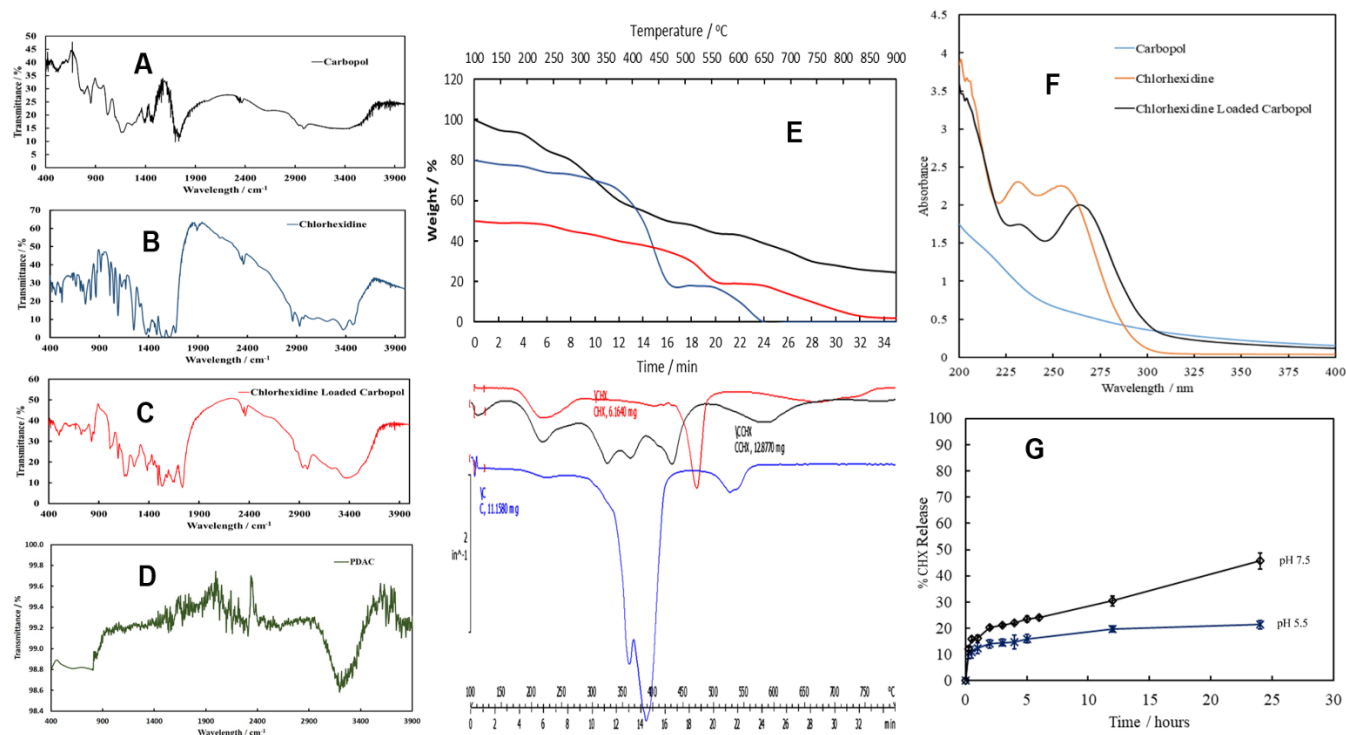


Figure 3. The Fourier Transform-IR spectrum of Carbopol Aqua SF1 (A), chlorhexidine (B), CLC (C) and PDAC (D). These materials were dried and mixed with excess of KBr pellets to prepared KBr discs for each of Carbopol nanogel, CHX and CLC which in turn were scanned individually from 400 cm^{-1} to 4000 cm^{-1} . (E) Thermal Gravimetric Analysis (TGA) and Differential Thermal Analysis (DTA) of chlorhexidine (red line), Carbopol Aqua SF1 (blue line) and CLC (black line) from 100 $^{\circ}\text{C}$ to 900 $^{\circ}\text{C}$ at 10 $^{\circ}\text{C}/\text{min}$ in air atmosphere with purge rate of 10 mL min^{-1} . (F) The UV/vis absorbance spectrum of 0.01 wt% Carbopol Aqua SF1 (Blue line), 0.007 wt% CHX (Orange line) and 0.006 wt% CLC (Black line). (G) The percentage of CHX release as a function of time for 0.15 wt% CHX-loaded in 0.1 wt% Carbopol (CLC). The experiment was conducted using 10 K MWCO dialysis bag filled up with 50 mL of CLC suspension. The whole dialysis bag was dipped in a beaker filled with 500 mL of either acetate buffer solution at pH 5.5 or phosphate buffer at pH 7.5. The CHX concentration in the buffer was monitored spectroscopically and calculated from Figure 2D.

The precipitate was washed twice with Milli-Q water and the supernatant discarded. 20 mL of Milli-Q water was added to the precipitate, the pH was gradually increased to 8 using drops of 0.25 M NaOH and the solution stirred overnight. The following morning the pH of the CHX-Carbopol (CLC) solution was reduced to 5.5 using acetate buffer. We measured the size distribution and zeta-potential of a range of solutions prepared by mixing aqueous solutions of different concentrations of CHX and the nanogel suspension. A Malvern Mastersizer was used to measure the CLC particle hydrodynamic diameter at a refractive index of 1.450. The pH was adjusted with 0.25 M HCl or 0.25 M NaOH solutions. Each value represents the average of a triple replicate with \pm S.D.

Release kinetics of CHX from CLC

We investigated the percentage of *in vitro* CHX released using aliquots of equivalent concentrations of CHX-loaded 0.1 wt% Carbopol nanogel. This formulation was optimized in terms of stability. The particle size and zeta potential of the CHX-loaded nanogel particles at pH 5.5 were 135 nm and -30 mV, respectively. The CHX-loaded nanogel suspension was placed into a dialysis cassette (10K MWCO, Thermo Fisher, UK) which released the CHX leaching from the nanogel through the membrane. The dialysis device was placed into a beaker which was already pre-filled with: (i) an acetate buffer solution at pH

5.5 or (ii) a phosphate buffer at pH 7.5 in order to monitor the amount of released CHX at a specific pH. The concentration of the released CHX was measured using UV-Visible spectrophotometer. All experiments were carried out in triplicate and the percentage of cumulative drug release was calculated.

Surface functionalization of CLC with PDAC

We used the cationic polyelectrolyte PDAC to reverse the surface charge of the Carbopol Aqua SF1 nanogel particles from negative to positive which promotes adhesion to the microbial cell walls. PDAC solutions with a range of different concentrations (0.001-0.01 wt%) were mixed separately with a fixed concentration of the nanogel (0.1 wt%) at a pH adjusted in the range of 4.75-5.00 using acetate buffer with the final volume of the suspension being 10 mL. The zeta potential was measured for each sample to find out the optimum concentration of both the PDAC and the nanogel which in turn give stable suspension. Typically, a 1.10 mL aliquot of 0.2 wt% PDAC solution was rapidly added to a suspension of 10 mL of the CLC suspension with vigorous shaking and then diluted to 20 mL to form PDAC-coated 0.005 wt% CHX-loaded 0.1wt% Carbopol Aqua SF1 nanogel dispersion (PDAC-coated CLC). The resulting solution was used as a stock to study its antimicrobial effect on *C. reinhardtii*, *S. cerevisiae*, *E. coli* and *S. aureus*.

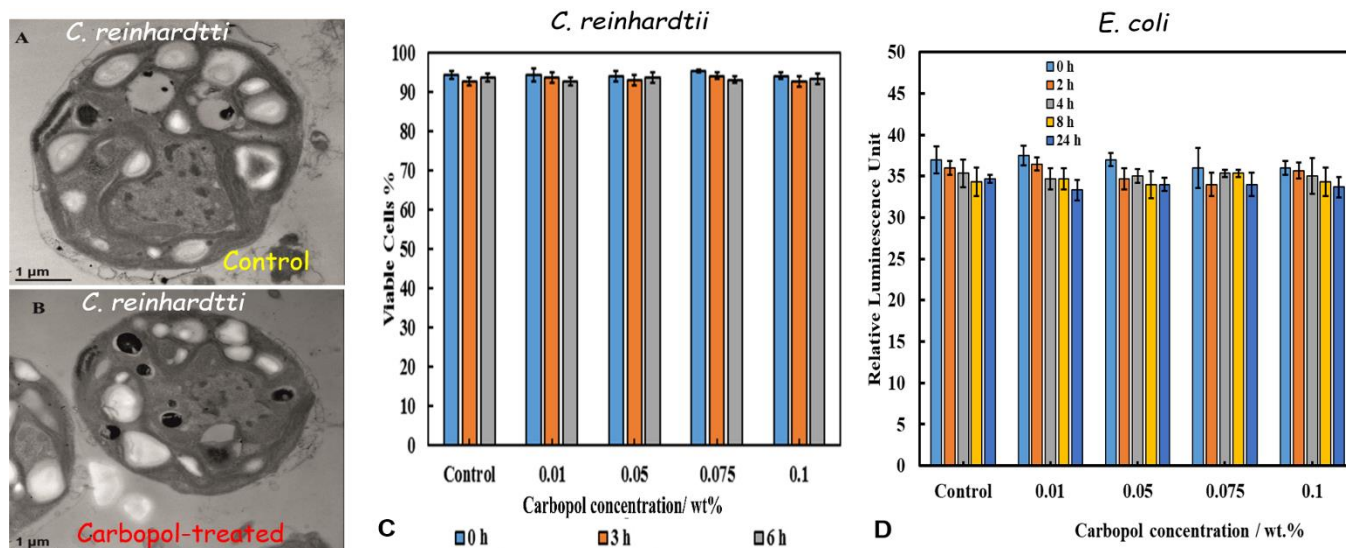


Figure 4. TEM images of sectioned *C. reinhardtii* cells (A) as control sample without prior treatment and (B) after incubation with 0.1% Carbopol Aqua SF1 nanogel followed by washing, negative staining and embedding in acrylic resin. The cell viability of *C. reinhardtii* (C) and *E. coli* (D) incubated in aqueous suspensions of varying concentrations of the nanogel at 25 °C at pH 5.5 for different periods of time. The cell viability was tested with FDA live/dead assay for *C. reinhardtii* and Promega CellTiter-Glo® assay for *E. coli*, respectively.

Cytotoxicity test of the non-coated Carbopol nanogel particles

A cell viability assay was performed to determine the cytotoxicity of the Carbopol Aqua SF1 nanogel on both of *C. reinhardtii* and *E. coli*. A 0.3 wt% dispersion of Carbopol Aqua SF1 was prepared in a 100 ml volumetric flask by dilution of an aliquot of the supplied stock with milli-Q water. The pH was adjusted to 5.5 using acetate buffer. 5 mL aliquots of the cell suspension were washed from the culture media and incubated with a series of 5 mL aliquots of the nanogel dispersion of concentrations (0.01–0.15 wt%) and tested at different incubation times. The control sample was treated in the same way without incubation with the nanogel. The cell viability was examined as described below.

Testing the effect of PDAC-coated CLC on *C. reinhardtii*

C. reinhardtii was cultured in media containing 2.42 g Tris, 25 mL TAP salts, 375 μ L phosphate solution, 1000 μ L Hunter's trace element, and 1000 μ L glacial acetic acid per 1 L of Milli-Q water. A 50 mL aliquot was removed from the culture for viability testing. This was centrifuged at 3000 rpm for 3 minutes to pellet the cells, the supernatant was discarded and the cells re-dispersed in 50 mL of fresh Milli-Q water by gentle shaking. Fluorescein diacetate (FDA) is a non-polar esterified compound which easily diffuses through the cell membranes. If the cell is viable and its membrane is intact the hydrolysis of the non-fluorescent precursor (FDA) by intracellular esterase leads to accumulation of fluorescein. We used 0.5% w/v FDA dissolved in acetone. 20 μ L of this solution was used per mL of cell sample. The tube with the mixture was shaken for 10 minutes using a vortex at 1500 rpm in dark conditions to avoid the photobleaching of the produced fluorescein inside the viable cells. This was repeated for cells incubated at room

temperature for 1 and 2 hours. The cell viability was measured using a Cellometer Auto X4 cell counter. 20 μ L of the sample was loaded into a disposable plastic counting chamber and the fluorescing (viable) and non-fluorescing (non-viable) cells measured using bright field and fluorescent microscopy imaging. This was repeated three times to obtain an average. When a cell viability above 85% was measured then the original 50 mL stock sample was used for further testing. 5 mL aliquots were of this stock were mixed with 5 mL aliquots of various treatments for 0 hours (5 minutes), 1 hour and 2 hours, respectively. We tested the *C. reinhardtii* cell viability in the following solutions:

- 0.005 wt% PDAC;
- 0.005 wt% PDAC-coated 0.1 wt% Carbopol (no CHX);
- 0.1 wt% CHX (chlorhexidine digluconate);
- 0.1 wt% encapsulated CHX in 0.1% Carbopol (CLC);
- 0.005 wt% PDAC - coated 0.1 wt% CHX-loaded in 0.1 % Carbopol (PDAC-coated CLC).

After incubation of the microalgae cell sample with these solutions, an aliquot was again centrifuged at 3000 rpm for 5 minutes and excess treatment washed away. The cells were re-suspended in 1 mL of Milli-Q water. *C. reinhardtii* cell viability was measured by using 20 μ L of this cell suspension in a Cellometer Auto X4.

Testing the effect of PDAC-coated CLC on *S. cerevisiae*

S. cerevisiae was cultured in media containing 20 g peptone, 10 g yeast extract, 20 g D-glucose per 1000 mL Milli-Q water. 0.01 g of dried *S. cerevisiae* was added per 100 mL of media. A 50 mL aliquot was removed from the culture for viability testing. This was centrifuged at 3000 rpm for 3 minutes to pellet the cells, the supernatant was discarded and the cells dispersed in 50 mL of fresh Milli-Q water by gentle shaking. 1 mL of washed

S. cerevisiae sample was pipetted into a sample tube and 20 μL of the FDA stock solution in acetone was added and the mixture was incubated at room temperature in dark conditions. This was repeated for cells incubated at room temperature for 1 hour and 2 hours. The viability was measured using a Cellometer Auto X4 cell counter as described previously for *C. reinhardtii*.

Testing the effect of PDAC-coated CLC on *E. coli*

We prepared 300 mL of *E. coli* cultured in LB media. 50 mL was aliquoted and subsequently centrifuged at 3000 rpm for 5 minutes. The supernatant was discarded, and the cell pellet re-suspended in 50 mL of milli-Q water. Various concentrations of treatment formulations were created in 5 mL aliquots (see Table 1) by dilution from the stock solution of 0.0025 wt% PDAC-coated 0.05 wt% CHX-Carbopol. 5 mL of the *E. coli* culture (redispersed in Milli-Q water) was added to 5 mL of the various formulations and gently shaken by hand to mix. The *E. coli* and formulation aliquots (total 10 mL) were incubated for 0 hours (5 min), 1 hour and 2 hours, respectively under the same conditions as for the original *E. coli* culture. Post incubation the *E. coli* and treatment aliquot was centrifuged at 3000 rpm for 5 minutes and the supernatant discarded (removing access CHX and halting the cell viability experiment). The cell pellet was resuspended in 1 mL of Milli-Q water by gentle shaking. 100 μL aliquot of each sample was pipetted into white opaque 96 well plate and immediately afterwards 100 μL Promega Cell Titer-Glo[®] luminescent cell viability assay reagent was added. The mixture of sample and reagent was equilibrated at room temperature for 30 minutes as stated in the manufacturer's protocol. The luminance was measured using a Thermo Scientific Fluroskan Ascent FL.

Protocol for SEM imaging of the treated cells

The microbial cells to be studied were removed from their culture media by washing PBS buffer, adhered to Aclar film, and then fixed in 2.5 wt% glutaraldehyde in 0.1M cacodylate buffer pH 7.2 for 2 hours at room temperature. Then, they were washed three times with cacodylate buffer and fixed in 1 wt% osmium tetroxide in cacodylate buffer for 1 hour. Finally, the cells were washed with cacodylate buffer, dehydrated in a series of ethanol-water solutions with decreasing water content and then dried using liquid carbon dioxide at its critical point.

MIC and MBC of CHX and PDAC-coated CLC on *S. aureus*

The following protocol was used to determine the Minimal Inhibitory Concentration (MIC) and the Minimal Bactericidal Concentration (MBC) of CHX and PDAC-coated CLC on *S. aureus*. A negative control of 100 μL of MHB (Muller Hinton Broth) was added to the first line of wells of a 96 well plate. 50 μL of MHB was added to the treatment wells and the positive bacteria control wells. A stock solution of CHX and PDAC-coated CLC was created in fresh MHB to a total volume of 10 mL. 50 μL of this formulation was added to the first line of treatment wells, and serially diluted 1:2 across the 96 well plate, ensuring it was mixed by pipetting up and down within each well. An overnight culture

of *S. aureus* was diluted into sterilised 0.85% saline until an absorbance reading of between 0.08-0.12 at 625 nm was obtained on a spectrophotometer (0.5 McFarland Standard). The saline diluted bacteria was diluted further 1:150 into MHB (10 mL MHB + 66.67 μL of bacteria in saline solution) yielding a 10 mL stock containing $5 \times 10^5 - 1 \times 10^6$ /mL cells. 50 μL from this bacteria stock was added to each treatment and positive bacteria control wells, seeding with $2.5 \times 10^4 - 5 \times 10^4$ cells per well. Each well contained a final volume of 100 μL with decreasing concentrations of treatment on equal amounts of bacteria. The plate was incubated for 20 hours at 37°C. After incubation, 20 μL of resazurin solution was added to each well, and the plate incubated for 3 hours at 37°C. The resazurin solution was formulated by dissolving resazurin powder into DPBS at 0.15 mg/mL. The plate was then colorimetrically measured at 570 nm excitation / 595 nm emission. The reading from the negative control wells was subtracted from the remaining wells to remove background absorbance. The MIC was determined by from the lowest concentration treatment which inhibited growth.

S. aureus time kill assay

Antimicrobial activity of 0.1% free CHX and 0.1% CHX-encapsulated in CLC after PDAC-functionalisation was tested against *S. aureus* (ATCC number 29213). An overnight culture of *S. aureus* was diluted in MHB to a population of $5 \times 10^5 - 1 \times 10^6$ CFU/mL, and treated with antimicrobial formulations at 37°C. At selected time points 100 μL aliquots were removed, neutralised in Dey-Engley Broth and serially diluted for colony enumeration. The control received no treatment. This was added to the 5 mL bacterial sample creating a 10 mL aliquot containing $5 \times 10^5 - 1 \times 10^6$ /mL CFU and 0.1 wt% CHX in 0.005 wt% PDAC-coated CLC encapsulated chlorhexidine. The three aliquots of were placed into a shaking rack and incubated at 37°C for 24 hrs. 100 μL (from the 10 mL test sample yields $5 \times 10^4 - 1 \times 10^5$ CFU/100 μL) of each of the aliquots were removed at specific time points, 0 hr, 30 min, 1, 2, 3, 6 and 24 hours. The 100 μL sample that was removed was serially diluted in neutralising Dey-Engley broth and plated onto agar at 10^2 , 10^3 , 10^4 , 10^5 , 10^6 , 10^7 dilutions depending on the time point (100 μL spread on agar x 3 repeats). The plates were incubated at 37 °C and enumerated 24 hours later.

Results and Discussion

Encapsulation of CHX into Carbopol Aqua SF1 nanogel

We used a pH mediated swelling/deswelling method to encapsulate CHX cations in the core of the acrylate copolymer nanogel particles. Figure 2A shows the increase of the nanogel particle size with the increase of pH. Here we enclose details of the swelling behaviour of the Carbopol nanogel before and after loading with CHX. The non-loaded Carbopol nanogel particles have an average diameter of about 100 nm at a pH below 6.8 and swells sharply to approximately 330 nm just above pH 7.

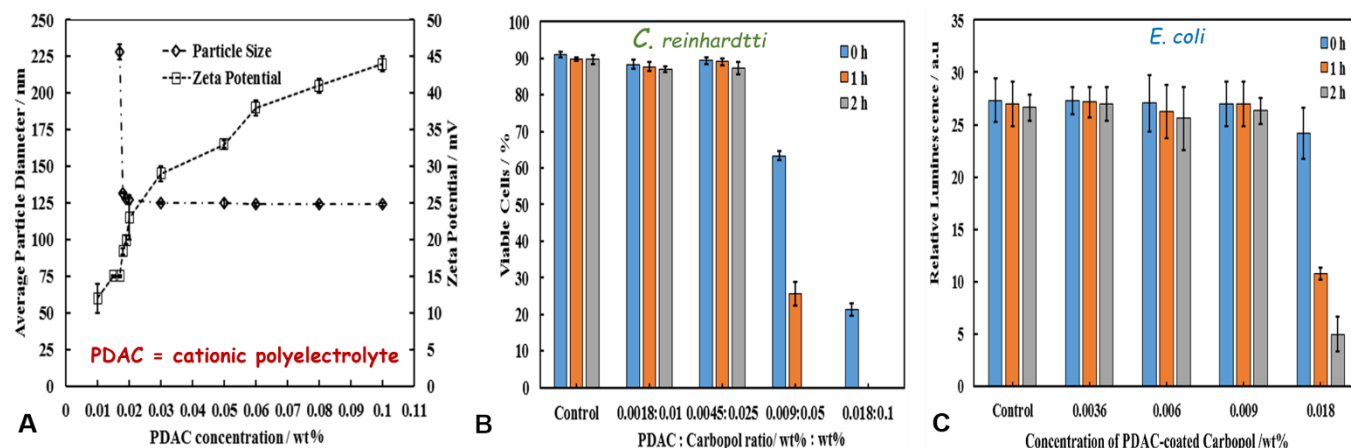


Figure 5. All data on this figure characterise the non-loaded Carbopol nanogel after coating with PDAC. (A) The average particle hydrodynamic diameter and zeta-potential of PDAC-coated Carbopol Aqua SF1 suspension as a function of the PDAC concentration which were obtained by mixing solutions of varying concentration of PDAC with 0.1 wt% Carbopol nanogel. The cytotoxic effect of PDAC-coated Carbopol Aqua SF1 particles at different ratios of PDAC-to-Carbopol on (B) *C. reinhardtii* and (C) *E. coli* for up to 2 hours at 25 °C.

The swelling/deswelling feature of the Carbopol microgel was exploited for the purposes of development of CHX delivery system. This microgel was therefore used to encapsulate chlorhexidine digluconate with the aim of targeted delivery to microbial cells. The size of the collapsed Carbopol nanogel particles was also confirmed by TEM imaging (Figure 2B). Above pH 7 the Carbopol Aqua SF1 nanogel particles swell as the carboxyl groups of the acrylate-copolymer are deprotonated to a higher degree which allows the CHX cations to interact and bind with them electrostatically. This was then followed by a pH drop to 5.5 which causes shrinkage of the CHX-loaded nanogel particles (CLC), which are then centrifuged to separate them from the free CHX. The pH of the CLC suspension was raised to pH 8 so that the particles in the pellet swell and re-disperse again. This was followed by de-swelling the redispersed particles at pH 5.5 using acetate buffer. This procedure yielded fully dispersed and stable suspension of CHX-loaded Carbopol nanogel. Figure 2C illustrates the visual appearance of the nanogel suspension at different stages of the loading with the CHX and their successful re-dispersing in water.

Effect of the CHX concentration on the CLC nanocarrier stability

After encapsulation of the CHX in the swollen nanogel particles and their shrinking at pH 5, the size of the loaded (CLC) particles depends on both the initial CHX and Carbopol concentration. The effect of different concentrations of chlorhexidine on the colloidal stability of the 0.1 wt% Carbopol Aqua SF1 was investigated. Figure 2E shows the increase of the nanogel particle size after loading with CHX. The particle size increase is an indication for partial aggregation at high CHX-to-Carbopol ratio. Therefore we choose to work at 0.1 wt% Carbopol initial concentration and a moderate CHX-to-Carbopol ratio as it only marginally increased the size of the collapsed CLC nanogel particles at pH 5.5 across the full range of CHX concentrations (Figure 2E). At higher CHX concentrations (0.1 wt%), the average

hydrodynamic diameter of the collapsed CLC particles appeared to be 135 nm without significant particle aggregation. The loading of the nanogel particles with CHX did not seem to significantly change the zeta potential of the collapsed CHX loaded nanogel (CLC) as a function of the CHX initial concentration, which remained negative in the range -25 – -30 mV (Figure 2E).

Spectroscopy studies of the CLC nanogel particles

FTIR spectra were obtained for Carbopol, CHX, CHX-loaded Carbopol (CLC). For Carbopol (Figure 3A), a characteristic peak was seen in the range 3300 – 3500 cm^{-1} due to the stretching vibrations of O-H and intermolecular hydrogen bonding. The strong peak between 2850 cm^{-1} and 3000 cm^{-1} is due to the stretching vibration band of the aliphatic C-H bond. The peak in the range 1670 – 1750 cm^{-1} is attributed to a strong vibration band of carbonyl stretching (C=O) while the two variable peaks at 1400 – 1490 cm^{-1} were assigned to the stretching vibration band of the carbonyl bond (C-O). The peak appearing from 1000 – 1300 cm^{-1} was attributed to the coupling between in-plane O-H bending and C-O stretching of neighbouring carboxyl groups.^{34,35} The spectrum of CHX (Figure 3B) is characterized by the main stretching vibrations from 3300 cm^{-1} to 3500 cm^{-1} for the N-H group. The bands at 2850 cm^{-1} to 3000 cm^{-1} are stretching vibration bands due to the aliphatic C-H group, while the peak at 1672 cm^{-1} relates to the stretching vibration band of the aliphatic C=N group which is considered as a characteristic peak of CHX. There are also peaks at wavelengths from 1450 cm^{-1} to 1550 cm^{-1} which are assigned to C=C group in the aromatic ring and at 1251 cm^{-1} which relates to the stretching vibration frequency of aliphatic amine (C-N) group.^{36–38} Figure 3C shows the FTIR spectrum of CLC. The broad absorption band at 3435 cm^{-1} can be allocated to the O-H groups for Carbopol while the band at 3364 cm^{-1} for the N-H group for chlorhexidine.

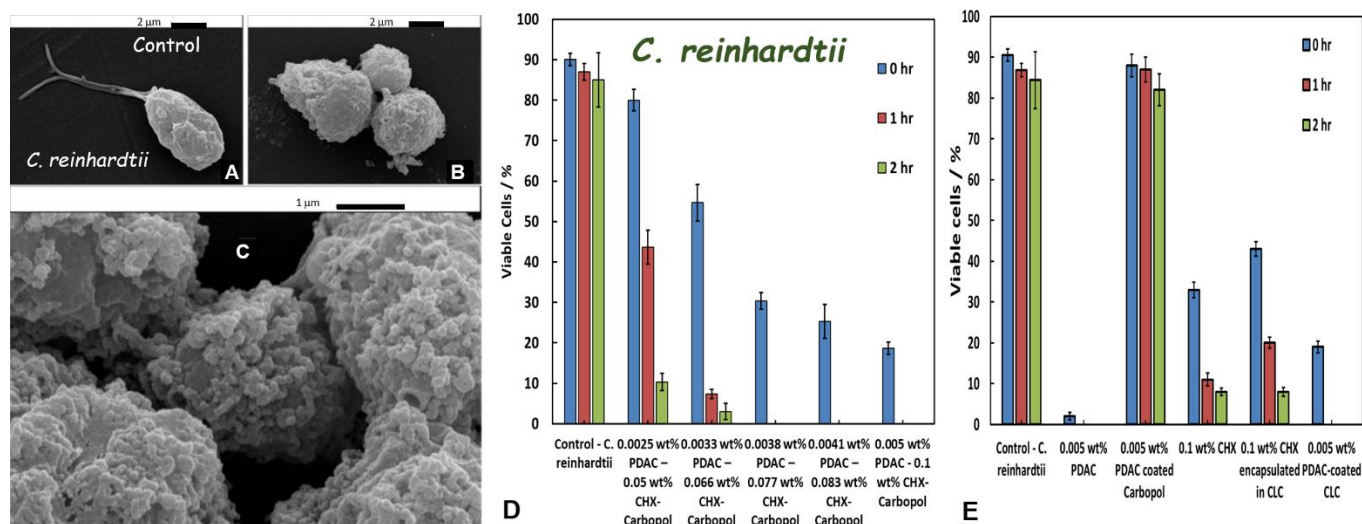


Figure 6. SEM images of *C. reinhardtii* cells with (A) being the control sample of untreated *C. reinhardtii*, (B) and (C) samples of *C. reinhardtii* after incubation in a suspension of 0.005 wt% PDAC-0.0225 wt% CHX-Carbopol Aqua SF1 suspension for 1 hour. (D) The viability of *C. reinhardtii* cells after timed exposure to antimicrobial formulations of PDAC-coated CLC at different concentrations for various time points (0, 1, 2 hours). The solutions are prepared by gradual dilution of a stock of 0.005 wt% PDAC-coated 0.1 wt% CHX loaded in 0.1 wt% Carbopol (CLC). (E) The viability of *C. reinhardtii* cells after timed exposure to antimicrobial formulations in Milli-Q water for various time points (0, 1, 2 hours). The graph compares the anti-algal activity of 0.005 wt% PDAC, 0.005 wt% PDAC coated Carbopol Aqua SF1 nanogel, 0.1 wt% CHX, 0.1 wt% CLC and 0.005 wt% PDAC-coated 0.1 wt% CLC. The cell viability was tested with FDA live/dead assay in a Cell counter.

The frequencies at 1653 cm^{-1} and 1734 cm^{-1} were noticed as principal characteristic bands for CHX-loaded Carbopol Aqua SF1 as they represent the vibration bands of the aliphatic C=N group for CHX and the carbonyl group (C=O) for Carbopol, respectively. The FTIR spectra therefore confirm that the CHX was successfully encapsulated into Carbopol Aqua SF1 nanogel. This result was also supported by TGA (Figure 3E) and the UV-vis spectrum data for CLC (Figure 3F). The UV-vis absorption spectrum of Carbopol Aqua SF1, CHX and CLC indicate the physical conjugation between Carbopol Aqua SF1 and CHX. It can be seen that Carbopol Aqua SF1 (blue line) absorbs in the UV region between 250 nm to 200 nm. CHX (orange line) has two broad absorbance peaks in the UV region, one at 254 nm and another at 233 nm. The CLC (black line) exhibited two substantial peaks at 264 nm and 233 nm confirming the presence of intercalated CHX into the Carbopol nanogel particles. The presence of PDAC was not possible to detect from the FTIR spectra of the PDAC-coated CLC as the PDAC is in negligible amount (Figure 3D). There are no characteristic peaks from PDAC on the FTIR spectrum of the PDAC-coated CLC. However, the zeta-potential measurements confirm its presence as it reverses from negative for CLC to positive (Figure 2E) upon coating with PDAC.

Elemental (CHN) analysis of CLC

Table 1 shows the wt% of C, H and N for Carbopol Aqua SF1 and CHX-loaded in Carbopol Aqua SF1 (CLC) per dry weight. The percentage of encapsulated CHX can vary depending on the initial CHX concentration used during the encapsulation process with the Carbopol nanogel. CHN-analysis data showed that the percentage of CHX into the CLC was about 13.2 wt% (per dry weight of CLC). The mole ratio of COOH-group (in Carbopol) to CHX was found to be about 50. In this estimate we have

assumed that the Carbopol composition corresponds to polyacrylic acid. This explains why the CHX-loaded Carbopol (CLC) particles still carry negative surface charge (negative zeta potential) which is due to the dominance of the nanogel COOH groups over the positive charge brought by the CHX.

Table 1. The elemental analysis of Carbopol Aqua SF1 and the encapsulated chlorhexidine (CHX) into Carbopol Aqua SF1 microgel through centrifuging and drying the each sample in air at room temperature.

Element	% in Carbopol Aqua SF1	% in CLC
C	56.73	53.59
H	4.99	7.35
N	0.00	3.67
The % drug content in Carbopol Aqua SF1		13.2
Mole Ratio (COOH/CHX)		50.2

Release kinetics of CHX from CLC

Our CHX release experiments done under sink conditions showed that the CLC nanogel particles can slowly release free CHX upon multiple dilution with water (see Figure 3G) over the course of 24 hours. The CHX release rate from the nanogel depends on the pH of the surrounding medium. At pH 5.5, approximately 13% of the encapsulated CHX was released after 2 hours while 17% of the total encapsulated amount was released after 5 hours. At pH 7.5, 20% of the CHX was released out of the nanogel after 2 hours and 25% after 5 hours. The sustained release of CHX from the nanogel particles could be beneficial in many antimicrobial applications where CHX concentration has to be supported in the surrounding media for a long period of time. The higher rate of release of CHX at the higher pH can be explained by the partial swelling of the nanogel which facilitates the CHX diffusion and intercalation within the particles interior.

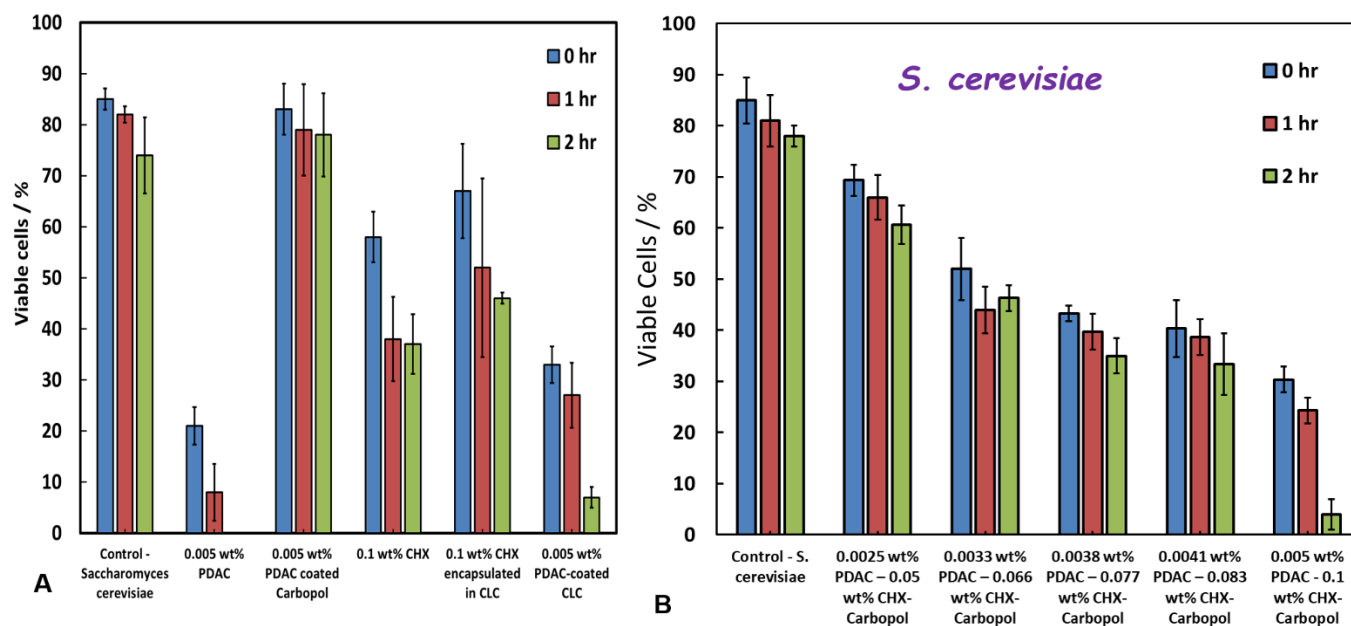


Figure 7. (A) The viability of *S. cerevisiae* cells after exposure to different antimicrobial formulations in Milli-Q water for several incubation times (0, 1, 2 hours). The graph compares the anti-yeast activity of 0.005 wt% PDAC, 0.005 wt% PDAC coated Carbopol Aqua SF1 nanogel, 0.1 wt% CHX, 0.1 wt% CLC and 0.005 wt% PDAC-coated 0.1 wt% CLC. (B) The viability of *S. cerevisiae* cells after exposure to formulations of PDAC-coated CLC at different concentrations for various incubation times (0, 1, 2 hours). The solutions are prepared by gradual dilution of a stock of 0.005 wt% PDAC-coated 0.1 wt% CHX loaded in 0.1 wt% Carbopol (CLC). The yeast cell viability was tested with FDA live/dead assay in a cell counter.

Toxicity assay of the non-coated Carbopol nanogel particles

Two test microorganisms, *C. reinhardtii* (microalgae) and *E. coli*, were incubated with Carbopol Aqua SF1 suspensions of different concentrations of nanogel particles. The cells were removed from the culture media to avoid any interaction between the nanogel particles and the components of culture media. The morphology of *C. reinhardtii* after incubation with the nanogel was studied by TEM. Figure 4B shows TEM images of sectioned microalgae cells after incubation for 24 hours with 0.1 wt% Carbopol nanogel at pH 5.5. The cell wall and the internal microstructure the Carbopol nanogel-treated microalgae do not indicate visible disruption compared with the control microalgae (Figure 4A). Cell viability assay (Figure 4C) does not indicate any cytotoxic effect of the non-loaded Carbopol Aqua SF1 on *C. reinhardtii* for a wide range of Carbopol Aqua SF1 concentrations at room temperature and up to 6 hours of incubation. Figure 4D also shows no pronounced cytotoxic effect of the Carbopol nanogel on *E. coli* cells for up to 24 hours. Similar results (not presented here) were also obtained for *S. cerevisiae*. These data are in agreement with the manufacturer's technical data for other microorganisms.³¹

Effect of PDAC-functionalization on Carbopol nanogel stability and toxicity

Figure 5A shows the average particle hydrodynamic diameter of the PDAC-coated Carbopol Aqua SF1 nanogels as a function of the PDAC-concentration. PDAC-coated Carbopol particles show good colloidal stability up to 0.03 wt% PDAC with zeta-potentials ranging from +12 mV for 0.017 wt% PDAC to +44 mV for 0.1 wt% PDAC at pH 5.5. This result shows that upon coating with PDAC, the surface charge of the Carbopol nanocarrier has

changed from negative (bare Carbopol) to positive giving cationic particles. We measured the zeta-potential of 0.005% PDAC-coated 0.1% carbopol over an interval of over 24 hours and did not find any measurable change, as it stayed around $+25 \pm 2$ mV at pH 5.5 (see Figure 2D). Figures 5B and 5C show the FDA viability assay for *C. reinhardtii* and *E. coli* upon incubation with the PDAC-coated nanogel without CHX. One can see that the nanocarrier shows measurable toxicity above 0.009 wt% PDAC for *C. reinhardtii* and above 0.018 wt% for *E. coli*. In order to distinguish between the toxicity of the PDAC-coating and the antimicrobial action of the CHX, we chose to work at concentrations of 0.005 wt% PDAC for which the "empty" nanocarrier is non-toxic to both microorganisms. Therefore, any further manifestation of antimicrobial action of 0.005 wt% PDAC-coated CLC would be solely due to delivery of CHX rather than effect of the PDAC coating of the nanocarrier.

Anti-algal action of PDAC-coated CLC on *C. reinhardtii*

The antimicrobial activity of CHX with *C. reinhardtii* was examined by incubation of the microalgae cells for up to 2 hours in PDAC-coated CHX-loaded Carbopol nanogel suspensions of different concentrations. Figures 6B and 6C shows SEM images of *C. reinhardtii* cells which have been incubated with a suspension of 0.005 wt% PDAC-0.0225 wt% CHX-0.1 wt% Carbopol for 1 hour. The SEM image in Figure 6A shows the morphology of the control sample of untreated microalgae. One can see that the cationic nanogel particles have accumulated on the cell wall of the treated microalgae. Figure 6C shows a high magnification SEM image which visualises the hetero-coagulation of the CHX-loaded nanocarrier on the cells.

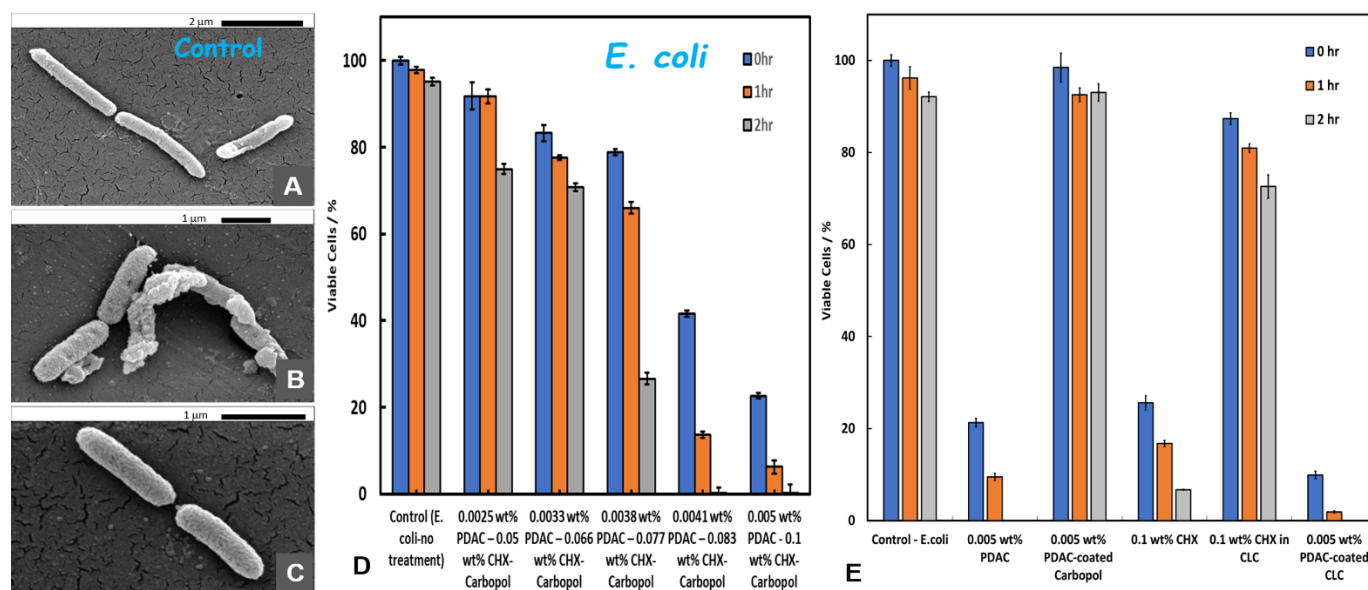


Figure 8. SEM images of *E. coli* cells after incubation in a suspension of PDAC-coated CLC for 2 hours at room temperature suspension. (A) The control sample of non-treated *E. coli*, (B) and (C) *E. coli* samples after treatment. (D) The viability of *E. coli* cells after timed exposure to antimicrobial formulations of PDAC-coated CLC at different concentrations for various time points (0, 1, 2 hours). The solutions were prepared by gradual dilution of a stock of 0.005 wt% PDAC-coated 0.1 wt% CHX loaded in 0.1 wt% Carbopol (CLC). (E) The viability of *E. coli* cells after exposure to various antimicrobial formulations in Milli-Q water for various time points (0, 1, 2 hours). The graph compares the antibacterial activity of 0.005 wt% PDAC, 0.005 wt% PDAC coated Carbopol Aqua SF1 nanogel, 0.1 wt% CHX, 0.1 wt% CLC (without PDAC coating) and 0.005 wt% PDAC-coated 0.1 wt% CLC. The bacterial cell viability was tested with Promega CellTiter-Glo® assay.

This clustering and accumulation of particles is attributed to the attraction between the PDAC-functionalised nanogel particle and anionic surface of the cells. As a result, the local release of CHX from the nanocarrier directly onto the cell membrane appears to increase its anti-algal action. Figure 6D shows the concentration dependence of the PDAC-coated CLC on the microalgae cell viability. The cells were incubated in a series of suspension obtained by multiple dilution of a stock suspension of 0.005 wt% PDAC-coated 0.1 wt% CHX-loaded 0.1 wt% Carbopol nanogel suspension. It can be seen that the CHX nanocarrier formulation containing a toxicity threshold concentration of 0.077 wt% (or higher) of encapsulated CHX reduced the microalgae viability from 90% to 0% after 1 hour of incubation. The original stock suspension completely killed the microalgae even after 1 hour of incubation and was able to reduce the microalgae viability from 90% to less than 20% even upon instant treatment (<5 min).

We also compared the efficiency of the PDAC-coated CLC with the equivalent concentrations of free CHX, non-coated CLC with the same concentration of CHX as well as the 0.005 wt% PDAC-coated nanocarrier without CHX and an equivalent concentration of free PDAC (0.005 wt%). The microalgae cell viability for all these samples and controls after up to 2 hours of incubation are compared with the viability of the untreated cells in Figure 6E. One sees that although free PDAC on its own has significant toxicity against the microalgae, the PDAC-coated nanocarrier (without CHX) does not show measurable toxicity when compared with the untreated control sample over the course of the experiment. Moreover, the results show that free CHX is more efficient in its anti-algal action compared with

equivalent amount of CLC. This can be explained by the fact that the CLC particles are negatively charged (Figure 2E) in the aqueous media and are electrostatically repelled from the negatively charged cell walls. However, the PDAC-coated CLC is not only more efficient than the non-coated CLC with the same amount of CHX but also it is also several times more effective than the treatment with the equivalent concentration of free CHX. This occurs because of the electrostatic attraction between the cationic PDAC-coated CLC and the anionic cell membrane of the microalgae which allows the released CHX to disrupt locally the cell membrane causing the cell death.

Anti-yeast activity of PDAC-coated CLC on *S. cerevisiae*

We tested the action of PDAC-coated CLC towards yeast cells. Figure 7A compares the yeast cells viability upon incubation for up to 2 hours with PDAC-coated CLC with equivalent concentration of free CHX, non-coated CLC with the same concentration of CHX as well as the 0.005 wt% PDAC-coated nanocarrier (without CHX) and the equivalent concentration of free PDAC (at 0.005 wt%). The results show that non-coated CLC is much less efficient than free CHX at the same concentration, which again is explained by the electrostatic repulsion between the yeast cell surface and negatively charged CLC particles, combined with the relatively slow release of CHX in the environment (cf. Figure 3F). One can also see from this comparison that the yeast cells are completely unaffected by the PDAC-coated Carbopol nanocarrier (without CHX), although it has significant loss of viability in the presence of free PDAC at the same concentration.

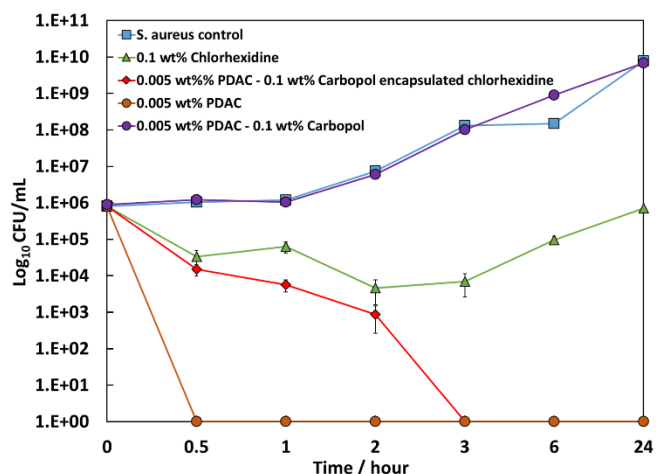


Figure 9. Time kill assay for chlorhexidine and 0.005 wt% PDAC-coated 0.1 wt% CHX loaded in 0.1 wt% Carbopol (CLC), 0.005 wt% free PDAC and 0.005 wt% PDAC-coated 0.1% Carbopol (empty nanocarrier) tested against *S. aureus*. The results are presented as means \pm SD ($n = 3$). Some of the error bars are within the symbol size. The lines are guides to the eye.

PDAC is a very efficient antimicrobial agent as it is a cationic polymer which tends to disturb the cell walls even at very low concentrations. However, PDAC-coated CLC showed much higher anti-yeast efficiency than free CHX and CLC at the same equivalent CHX concentration. The explanation for this enhanced antimicrobial effect is related to the heterocoagulation of the positively charged PDAC-coated CLC on to the negatively charged cell walls which boosts the local CHX concentration directly on the yeast cells surface. Comparing Figure 6D with Figure 7A one can see that under the same condition the PDAC-coated CLC is more efficient against the microalgae than against yeast, which can be attributed to the much thicker cell wall of the yeast cells. In both cases of yeast and microalgae we observe a better antimicrobial action of the PDAC-coated CLC than free CHX and non-coated CLC. Figure 7B shows the concentration dependence of the anti-yeast action for a stock suspension of 0.005 wt% PDAC-coated 0.1 wt% CHX – loaded in 0.1% Carbopol. The yeast cell viability was measured after up to 2 hours of incubation in solutions obtained by multiple dilution of this stock suspension of PDAC-coated CLC particles. The yeast cell viability can be seen to have reduced from 85% to less than 5% after 2 hours of incubation in the stock suspension, compared with 77% viability for the untreated yeast. The comparison of Figure 7B with Figure 6D also confirms that yeast is more resistant towards the PDAC-coated CLC than the microalgae.

Anti-bacterial action of PDAC-coated CLC on *E. coli*

The antibacterial activity of PDAC-coated CLC with *E. coli* was investigated by incubation for up to 2 hours at room temperature with a fixed amount of *E. coli* cells removed from their culture media. Representative SEM images of the control sample of untreated *E. coli* are shown in Figure 8A, compared with *E. coli* samples treated with PDAC-coated CLC (Figures 8B and 8C). One can see that as with the microalgae (Figure 6B and

6C), the *E. coli* cells have become densely coated with the PDAC-functionalised CLC nanoparticles after exposure to the nanocarrier suspension. The result of this accumulation of the CHX-delivery vehicle on the cell viability was assessed in Figure 8D for various concentrations of the PDAC-coated CLC, obtained by gradual dilution of the stock of 0.005 wt% PDAC-coated 0.1 wt% CHX – loaded in 0.1% Carbopol.

It should be noted that the threshold of toxicity of the PDAC-coated CLC against *E. coli* is significantly lower than the one for yeast (cf. Figure 7B) but it is higher than for microalgae (cf. Figure 6D). Figure 8E compares the *E. coli* cells viability upon incubation with PDAC-coated CLC and solutions with equivalent concentration of free CHX, non-coated CLC with the same concentration of CHX, 0.005 wt% PDAC-coated “empty” Carbopol nanocarrier and free PDAC at the same concentration (0.005 wt%). A very similar picture emerges from this comparison, as the equivalent results with microalgae (Figure 6E) and yeast (Figure 7A). The PDAC-coated CLC shows much higher antibacterial efficiency against *E. coli* than both free CHX and non-coated CLC at the same equivalent concentration of CHX. Again, the empty PDAC-coated nanocarrier is benign for *E. coli*, i.e. the coating alone does not contribute to any loss of *E. coli* cell viability.

Antibacterial action of PDAC-coated CLC on *S. aureus*

We determined the MIC and MBC of free CHX and PDAC-coated CLC on *S. aureus* as a common bacterial culture found in isolates from hospital acquired infected wounds. We found that at the same conditions the MIC of the PDAC-coated CLC is 2 times lower than this of free CHX. The MBC of the PDAC-coated CLC is about 8 times lower than that of free CHX (see Table 2). These results illustrate the effect of the nano-encapsulation of the CHX into the Carbopol carrier and the targeted delivery of this antimicrobial agent directly on the surface for *S. aureus*, which requires several times lower overall CHX concentration to achieve the same effect as with free CHX. The advantages of this enhancement of the CHX antibacterial action is several fold. This means that the same level of bacterial growth inhibition can be achieved with 2 times lower CHX concentration and 8 lower minimal concentration of CHX encapsulated in CLC is needed for bactericidal action. Lowering the antimicrobial agent concentration in both cases can be beneficial from the point of view of economy of active material and lowering the overall side toxicity of the antibacterial formulation. This can be beneficial to reduce development of future bacterial resistance. Similar is the amplification effect of the PDAC-coated CLC on *E. coli*, *C. reinhardtii*, and *S. cerevisiae* compared with free CHX (Table 2). We also performed a comparative time kill assay on *S. aureus* using the same formulations of free CHX and PDAC-coated CLC at the same overall concentration of CHX. The result is presented on Figure 9 along with the control of untreated bacteria. One sees that the PDAC-coated CLC has practically achieves >5 log reduction within 3 hours while the formulation based on free CHX has only time-limited effect on the growth of *S. aureus*.

Table 2. Minimum inhibitory concentration (MIC) and minimum bactericidal/fungicidal concentration (MBC/MFC) of free CHX and PDAC-coated CLC against *S. aureus*, *E. coli*, *C. reinhardtii*, and *S. cerevisiae*. The lowest concentration of antimicrobial agent inhibiting/no growth was considered the MIC/MBC/MFC.

	CHX		PDAC-coated CLC	
	MIC	MBC	MIC	MBC
<i>S. aureus</i>	2.5 µL/mL (0.05 wt%)	10 µL/mL (0.2 wt%)	1.25 µL/mL (0.025 wt%)	1.25 µL/mL (0.025 wt%)
<i>E. coli</i>	5 µL/mL (0.1 wt%)	20 µL/mL (0.4 wt%)	2.5 µL/mL (0.05 wt%)	2.5 µL/mL (0.05 wt%)
<i>C. reinhardtii</i>	5 µL/mL (0.1 wt%)	5 µL/mL (0.1 wt%)	0.625 µL/mL (0.0125 wt%)	0.625 µL/mL (0.0125 wt%)
<i>S. cerevisiae</i>	5 µL/mL (0.1 wt%)	10 µL/mL (0.2 wt%)	1.25 µL/mL (0.025 wt%)	2.5 µL/mL (0.05 wt%)

Conclusions

We have developed a novel surface functionalized nanocarrier for chlorhexidine based on lightly cross-linked acrylate copolymer nanogel particles (Carbopol Aqua SF1). This nanocarrier was surface-functionalised by coating with the cationic polyelectrolyte PDAC and showed a strong enhancement of the chlorhexidine antimicrobial action. We explored the effect of these CHX-loaded nanocarrier on *C. reinhardtii* microalgae, *S. cerevisiae* and *E. coli* for CHX-loaded nanogel (CLC) with and without coating with the cationic polyelectrolyte (PDAC-coated CLC). We demonstrated that the cationic coating of the nanogel strongly amplifies the antimicrobial action of the loaded CHX against both *C. reinhardtii*, *S. cerevisiae* and *E. coli* even for short incubation times. The boost of the CHX antimicrobial activity was attributed to the favourable electrostatic attraction between the positively charged PDAC-coated CLC and the negatively charged cell membranes which leads to their attachment on the microbial cell walls where they release locally of highly concentrated CHX causing the cell death. SEM images of nanocarrier-treated cells showed the preferential deposition of the PDAC-coated CLC onto the cell membranes of all studied microbial cells. This type of very efficient cationic surface-functionalised nanogel carriers can be potentially applied to boost the antimicrobial action for a range of low-molecular weight cationic anti-fungal and anti-algal agents. Similar strategy could also find applications for enhancing the action of topical antibiotics and antifungal agents and may be used across different therapies to bypass antimicrobial resistance.

Acknowledgements

M.A. thanks the Iraqi Government, the Higher Committee for Education Development of Iraq and the Green University of Qasim, Babylon, Iraq for the financial support for his PhD study. P.J.W. is funded by a University of Hull Advanced Wound Care PhD cluster studentship.

ORCID IDs

Mohammed J. Al-Awady: 0000-0002-0506-6733

Paul J. Weldrick: 0000-0002-1791-5659
 Matthew J. Hardman: 0000-0002-6423-5074
 Gillian M. Greenway: 0000-0003-1873-8188
 Vesselin N. Paunov: 0000-0001-6878-1681

Notes and references

- K. S. Soppimath, T. M. Aminabhavi, A. R. Kulkarni and W. E. Rudzinski, *J. Controlled Release*, 2001, **70**, 1-20.
- P. S. Ayyaswamy, V. Muzykantor, D. M. Eckmann and R. Radhakrishnan, *J. Nanotechn. in Eng. and Medicine*, 2013, **4**, 011001.
- N. B. Graham and A. Cameron, *Pure and Appl. Chem.*, 1998, **70**, 1271-1275.
- N. A. Peppas, Y. Huang, M. Torres-Lugo, J. H. Ward and J. Zhang, *Ann. Review of Biomed. Eng.*, 2000, **2**, 9-29.
- D. Caccavo, S. Cascone, Sara; G. Lamberti, A. Barba, A. Anna Chem. Soc. Rev., 2018, **47**, 2357-2373.
- S. Liu, R. Maheshwari and K. L. Kiick, *Macromolecules*, 2009, **42**, 3-13.
- W. Shen, Y. Chang, G. Liu, H. Wang, A. Cao and Z. An, *Macromolecules*, 2011, **44**, 2524-2530.
- H. Urakami, J. Hentschel, K. Seetho, H. Zeng, K. Chawla and Z. Guan, *Biomacromolecules*, 2013, **14**, 3682-3688.
- D. Foulkes, *J. Periodontal Res.*, 1973, **8**, 55-60.
- G. Greenstein, C. Berman and R. Jaffin, *J. Periodontology*, 1986, **57**, 370-377.
- M. P. Young, D. H. Carter, H. V. Worthington, J. F. McCord, M. Korachi and D. B. Drucker, *Clinical Oral Implants Res.*, 2002, **13**, 20-29.
- C. Estrela, R. G. Ribeiro, C. R. Estrela, J. D. Pécora and M. D. Sousa-Neto, *Brazilian Dental J.*, 2003, **14**, 58-62.
- J. F. Siqueira, I. N. Rôças, S. S. Paiva, T. Guimarães-Pinto, K. M. Magalhães and K. C. Lima, *Oral Surgery, Oral Medicine, Oral Pathology, Oral Radiology and Endodontology*, 2007, **104**, 122-130.
- M. Bral and C. Brownstein, *Dental Clinics of North America*, 1988, **32**, 217-241.
- N. Lang and M. C. Brex, *J. Periodontal Res.*, 1986, **21**, 74-89.
- H. Löe and C. Rindom Schiøtt, *J. Periodontal Res.*, 1970, **5**, 79-83.
- N. Lavoine, N. Tabary, I. Desloges, B. Martel and J. Bras, *Colloids and Surfaces B: Biointerfaces*, 2014, **121**, 196-205.
- C. J. Seneviratne, K. C.-F. Leung, C.-H. Wong, S.-F. Lee, X. Li, P. C. Leung, C. B. San Lau, E. Wat and L. Jin, *PLoS One*, 2014, **9**, e103234.1-7.
- H.C. Stuart, S.A. Schwartz, T.J. Beeson, C.B. Owatz, *J. endodontics*, 2006, **32**, 93-98.
- I. C. Yue, J. Poff, M. a. E. Cortés, R. D. Sinisterra, C. B. Faris, P. Hildgen, R. Langer and V. P. Shastri, *Biomaterials*, 2004, **25**, 3743-3750.
- B. Jiang, G. Zhang and E. M. Brey, *Acta biomaterialia*, 2013, **9**, 4976-4984.
- H. Lboutounne, J.-F. Chaulet, C. Ploton, F. Falson and F. Pirot, *J. Controlled Release*, 2002, **82**, 319-334.
- M. E. Barbour, S. E. Maddocks, N. J. Wood and A. M. Collins, *Internat. J. Nanomedicine*, 2013, **8**, 3507-3519.
- A.F. Halbus, T.S. Horozov, V.N. Paunov, *Adv. Colloid Interf. Sci.*, 2017, **249**, 134-148.

25. A.A.K. Das and V.N. Paunov, *Microbiologist*, June 2014, pp.16-19. https://issuu.com/societyforappliedmicrobiology/docs/2014_06_micro_biologist
26. M.J. Al-Awady, G.M. Greenway, V.N. Paunov, *RSC Adv.*, 2015, **5**, 37044–37059.
27. M.J. Al-Awady, A. Fauchet, G.M. Greenway, V.N. Paunov, *J. Mater. Chem. B*, 2017, **5**, 7885-7897.
28. C. Frangville, M. Rutkevicius, A.P. Richter, O.D. Velev, S.D. Stoyanov, V.N. Paunov, *ChemPhysChem*, 2012, **13**, 4235–4243.
29. A.P. Richter, J.S. Brown, B. Bharti, A. Wang, S. Gangwal, K. Houck, E.A. Cohen Hubal, V.N. Paunov, S.D. Stoyanov, O.D. Velev, *Nat. Nanotechnol.*, 2015, **10**, 817–823.
30. A.P. Richter, B. Bharti, H.B. Armstrong, J.S. Brown, D. Plemmons, V.N. Paunov, S.D. Stoyanov, O.D. Velev, *Langmuir* 2016, **32**, 6468–647.
31. C. A. Lubrizol, Noveon Consumer Specialties, Technical Data Sheet, 2007, 294.
32. D. S. Gorman and R. Levine, *Proc. Natl. Acad. Sci. U. S. A.*, 1965, **54**, 1665–1669.
33. S. Hutner, L. Provasoli, A. Schatz and C. Haskins, *Proc. Am. Philos. Soc.*, 1950, **94**, 152–170.
34. S. Sahoo, C. K. Chakraborti and S. C. Mishra, *J. Adv. Pharm. Techn. & Res.*, 2011, **2**, 195-204.
35. M. Moharram and M. Khafagi, *J. Appl. Polym. Sci.*, 2007, **105**, 1888-1893.
36. A. Kovtun, D. Kozlova, K. Ganesan, C. Biewald, N. Seipold, P. Gaengler, W. H. Arnold and M. Epple, *RSC Advances*, 2012, **2**, 870-875.
37. K. Garala, P. Joshi, M. Shah, A. Ramkishan and J. Patel, *Internat. J. Pharm. Investig.*, 2013, **3**, 29-41.
38. P. Larkin, *Infrared and Raman spectroscopy; principles and spectral interpretation*, Elsevier, 2011.
39. A. Muñoz-Bonilla, M. Fernández-García, *Eur. Polymer J.*, 2015, **65**, 46-62.
40. A. Muñoz-Bonilla, M. Fernández-García, *Prog. Polymer Sci.*, 2012, **37**, 281-339.